Available online at www.sciencedirect.com
SCIENCE DIRECT®
Journal of Nuclear Materials 347 (2005) 307–313
journal of nuclear materials
www.elsevier.com/locate/jnucmat

Microstructural analysis on helium retention of ion-irradiated and annealed tungsten foils

N. Hashimoto [a,*], J.D. Hunn [a], N. Parikh [b], S. Gilliam [b], S. Gidcumb [b], B. Patnaik [b], L.L. Snead [a]

[a] *Oak Ridge National Laboratory, Metals and Ceramics Division, P.O. Box 2008, Building 4500S, MS 6136, Oak Ridge, TN 37831-6136, United States*
[b] *University of North Carolina at Chapel Hill, Chapel Hill, NC 27599-3255, United States*

Abstract

The helium retention characteristics and helium bubble distribution in tungsten were studied using $^3He(d,p)^4He$ nuclear reaction analysis (NRA) and transmission electron microscopy (TEM) on two forms of tungsten: single crystal and polycrystalline, implanted to 1×10^{19} $^3He/m^2$ at 850 °C and annealed at 2000 °C. The NRA results revealed that as-implanted single crystal and polycrystalline tungsten exhibited similar helium retention characteristics. Stepwise annealing reduced the helium retention in both single crystal and polycrystalline tungsten when the number of implantation steps and annealing time were increased. The TEM results indicated that microstructure played a large role in helium trapping; the existence of grain boundaries led to significant cavity formation and greater cavity growth. Single crystal tungsten had less trapping sites for helium, allowing long range He diffusion during annealing. The decrease of He retention in polycrystalline tungsten during stepwise annealing was probably due to significant recrystallization, resulting in decrease of grain boundary density.

1. Introduction

In an inertial fusion energy (IFE) reactor chamber, the tungsten armor on the first wall will be subjected not only to X-rays and neutrons, but also to significant ion fluxes. These fluxes vary in type, energy, and intensity and fall into roughly two categories: High-energy ions in the 1–10s of MeV range (C, ^4He) and ions in the 0.1–1 MeV range (He, D, T, H). While the chamber designs to date have focused on evaporative losses of first wall or armor due to the impinging X-ray flux from the target fusion, they have largely ignored degradation of mechanical properties due to neutron or ion induced compositional change and displacement damage as well as losses of material at the surface due to sputtering (chemical and physical), blistering, and exfoliation. The present paper focuses on potential damage arising from the helium ion flux.

The most deleterious ions are helium (and hydrogen, with potential synergistic effects) in the energy range 0.1–1 MeV, for which the stopping range is

* Corresponding author. Tel.: +1 865 576 2714; fax: +1 865 574 0641.
E-mail addresses: hashimoton@ornl.gov (N. Hashimoto), nparikh@physics.unc.edu (N. Parikh).

0022-3115/$ - see front matter © 2005 Elsevier B.V. All rights reserved.
doi:10.1016/j.jnucmat.2005.08.010

on the order of 0.1–1 μm. These ions cause formation of blisters with skin thickness on the order of 0.1–1 μm as well, and hence exfoliation of μm thick layers occurs above a threshold fluence. Studies on ceramics [1] and metals [2–4] show that blistering occurs in all He-implanted materials at room temperature and fluences around $\sim 3 \times 10^{21}$ m^{-2}, and exfoliation occurs for fluences around $\sim 10^{22}$ m^{-2}. These critical fluences decrease with increasing temperature. The critical fluence also increases slightly with increasing penetration depth (ion energy), due to range straggling effects. For a He flux of $\sim 2 \times 10^{18}$ m^{-2} s this implies that an exfoliation layer equal to the range of the He ions (~1 μm for the 1 MeV He ions) would form about once per hour and a surface erosion loss of about ~1 cm per year would result for the 1 MeV He ions. At 100% duty factor, this is equal to a surface erosion loss of ~2 cm per year. This implies that the He ions should be stopped from reaching the bare wall in order to avoid unacceptable wall erosion.

In an IFE chamber (drywall option), the tungsten first wall ($T_M = 3410$ °C) is expected to reach ~2500 °C for ~1 μs after each pulse. Helium ion bombardment creates vacancies within W that trap He and act as nucleation sites for He bubble growth. Considerable data are available on blistering due to low energy He ion implantation near room temperature [5]. Trapped He concentration and bubble sizes increases with dose and irradiation temperature due to increasing defect density and thermal mobility. At room temperature, growth of He bubbles beneath the surface causes blistering and surface exfoliation. The critical doses decrease with temperature and increase with ion energy (in ~1–2 MeV He range). However, there is insufficient information on the effects for pulsed implantation and anneal conditions for tungsten.

Helium retention characteristics and helium bubble distribution in tungsten were studied using ^{3}He(d,p)^{4}He nuclear reaction analysis (NRA), transmission electron microscopy (TEM) and scanning electron microscopy (SEM). Two forms of tungsten were used, single crystal and polycrystalline, implanted with to 1×10^{19} ^{3}He/m^2 and annealed at 2000 °C.

2. Experimental

Two forms of tungsten were used in this study: single crystal and polycrystalline. They were implanted at 850 °C with 1.3 MeV ^{3}He (range is ~1.67 μm, obtained from TRIM code) to 1×10^{19} ^{3}He/m^2 (flux was 1×10^{15}–10^{16} ^{3}He/m^2 s) at the University of North Carolina at Chapel Hill. Nuclear reaction analysis (NRA) using the ^{3}He(d,p)^{4}He reaction [6] was performed to analyze the ^{3}He content in the implanted specimens. Deuterons of 780 keV incident on W foils implanted with ^{3}He at a depth of 1.7 μm produces a spectrum of ~13 MeV protons, alphas, and backscattered deuterons. Due to overlap of the energy spectra of alphas and backscattered deuterons, the use of alphas for profiling ^{3}He was not possible. Mylar foils were used to stop the lower energy alphas and backscattered deuterons, but allowed transmission of the higher energy protons. Fig. 1 shows the resulting spectrum from NRA, indicating the higher energy proton peak from the ^{3}He(d,p)^{4}He reaction and other peaks at low energy from a reaction on the surface [7]. After implantation and NRA, flash annealing at ~2000 °C was performed for each

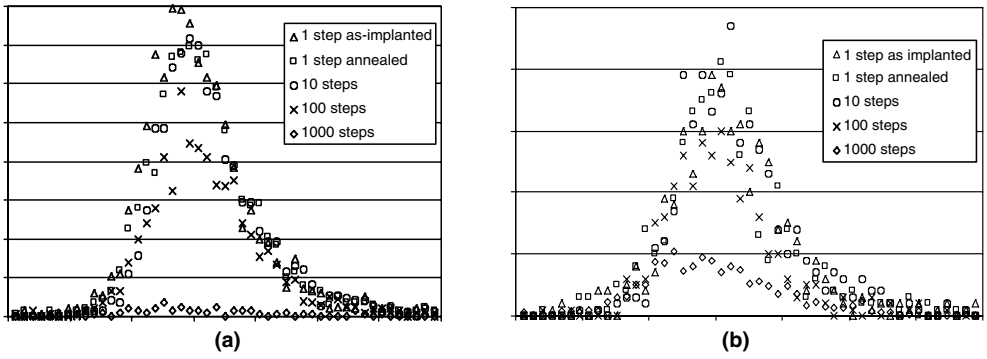

Fig. 1. Proton spectra for (a) single crystal and (b) polycrystalline tungsten implanted at 850 °C and flash annealed at 2000 °C in 1, 10, 100, and 1000 cycles to reach a total dose of 10^{19} He/m^2. The sample implanted with the total dose in one cycle was analyzed before and after the 2000 °C anneal [7].

specimen. The flash annealing consisted of heating to 2000 °C within 5 s, annealing at 2000 °C for 2 s, and cooldown to 850 °C in 5 s. Also, implantation in small steps with annealing between steps was performed using a computer automated system that allowed for 1000 step runs to be completed in 30 h. TEM specimens were prepared using focused ion beam micromachining (FIB). The FIB used a focused ion beam for controlled removal of material by sputtering. The FIB preparation involved sputter-coating the sample with Pt then depositing a thick protective layer of Pt using the FIB. Machining of the TEM specimen was then performed using 30 keV Ga^+ ions.

3. Results

3.1. Nuclear reaction analysis (NRA)

Fig. 1 shows He retention profiles of the single crystal and polycrystalline tungsten implanted with 10^{19} He/m^2 at 850 °C with intermittent annealing at 2000 °C [7]. In this experiment, '1 step' means annealing just once after implantation with 10^{19} He/m^2 and '100 steps' and '1000 steps' denotes annealing after each implantation of 10^{17} or 10^{16} He/m^2 and repeating this cycle 100 or 1000 times, respectively. The larger number of steps better simulate the condition of an IFE chamber. As seen in Fig. 1, as-implanted single crystal and polycrystalline tungsten exhibited similar helium retention characteristics. In addition, a flash anneal at 2000 °C had no effect on the retention of helium. It also appears that stepwise annealing reduces the helium retention for 100 steps and even more for 1000 steps. Actually, He implantation in 1000 cycles resulted in a decrease of the retained helium by 95% of the implanted amount for single crystal compared to 70% of that for polycrystalline tungsten. This result suggests a preference for single crystal over polycrystalline tungsten due to less He retention. For this implantation condition neither specimen showed any blistering nor/or exfoliation.

3.2. Microstructural analysis

3.2.1. Single crystal tungsten

Fig. 2(a) and (b) shows microstructures (cross section views) of single crystal tungsten implanted with 10^{19} He/m^2 at 850 °C followed by annealing at 2000 °C in a single step and in 1000 steps, respectively. No precipitates were observed in either case. Fig. 2(a) shows many tiny cavities (2–3 nm in diameter). The cavity distribution seemed to correspond to the profile of helium retention. Large numbers of cavities were distributed at a depth of 1.67 μm from the surface. In this implanted condition, no cavities were observed in the region from the surface to 1 μm depth. In contract, no visible cavities were observed in the 1000 step annealed single crystal, shown in Fig. 2(b). This observation is in good agreement with the NRA result (Fig. 1).

3.2.2. Polycrystalline tungsten

Fig. 3 shows the microstructures of polycrystalline tungsten implanted with 10^{19} He/m^2 at 850 °C

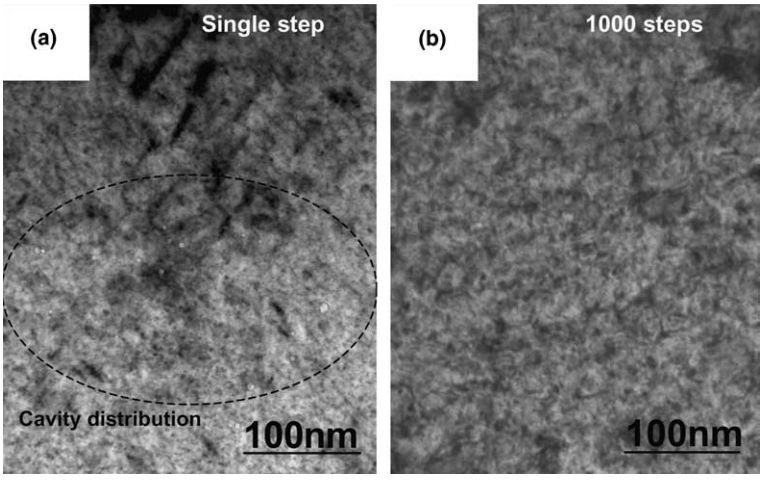

Fig. 2. Microstructures (cross section view) of single crystal tungsten implanted with 10^{19} He/m^2 at 850 °C followed by annealing to 2000 °C in (a) single step and (b) 1000 steps.

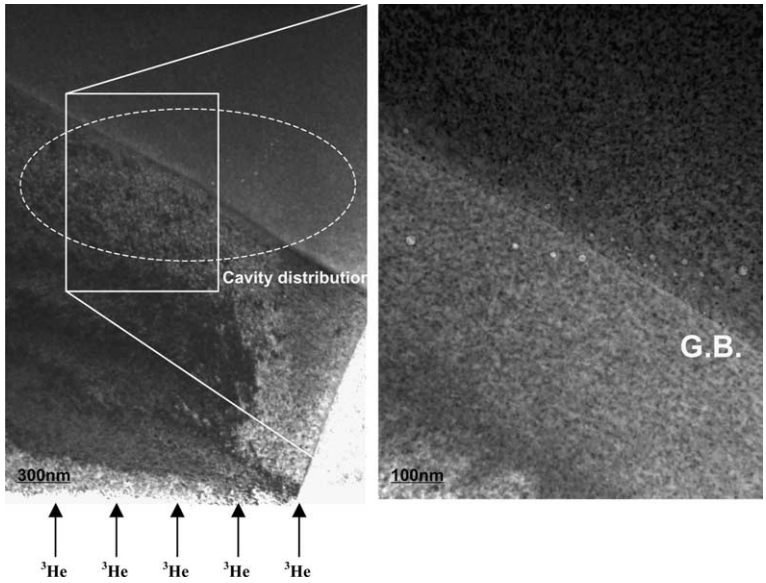

Fig. 3. Microstructures of polycrystalline tungsten implanted with 10^{19} He/m^2 at 850 °C followed by annealing at 2000 °C in single step.

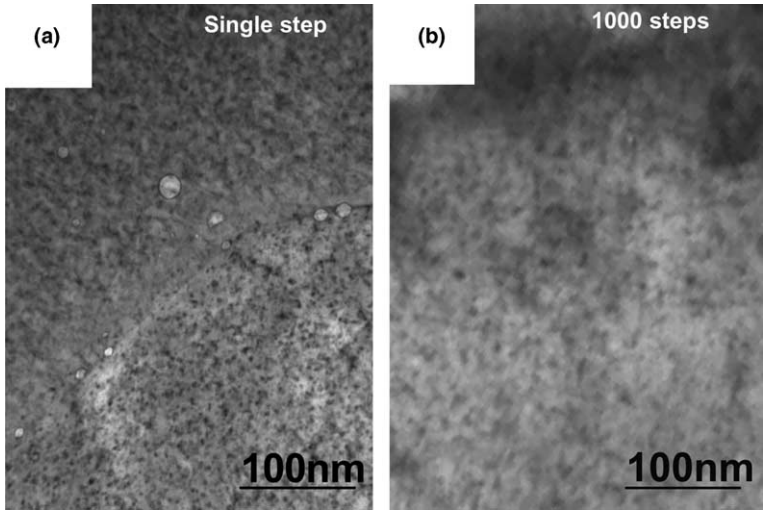

Fig. 4. Microstructures (cross section view) of polycrystalline tungsten implanted with 10^{19} He/m^2 at 850 °C followed by annealing to 2000 °C in (a) single step and (b) 1000 steps.

followed by annealing at 2000 °C in single step. No precipitate was observed in this cases. Single step annealing led to significant cavity growth at grain boundaries, which act as nucleation sites for He bubbles. Cavities were distributed at a depth of 1.0–1.8 μm from the surface. Fig. 4 compares microstructures of polycrystalline tungsten He-implanted and annealed (a) in a single step and (b) in 1000 steps. Annealing in 1000 steps resulted in no visible cavity formation even though the NRA results found polycrystalline tungsten had more He retention than single crystal tungsten. One possible reason is that the amount of helium retention in polycrystalline tungsten during 1000 steps annealing was not enough to form visible cavities (at least 1 nm in diameter).

4. Discussion

In general, helium diffusion in a metal matrix is strongly influenced by traps. These traps may be atomic scale defects like impurities and vacancies

or extended defects like dislocations, solid precipitates and He bubbles formed at interfaces or in the matrix. It is well known that helium drastically enhances the formation of cavities due to the strong interaction with lattice defects, vacancies and vacancy clusters [8–11]. In order to understand helium retention and/or cavity distribution in tungsten, it is important to have an idea of the cavity development in the grain interior as a function of He generation rate, He content, temperature, time and microstructure. In this experiment, the total helium content, implantation temperature and annealing temperature are constant, while He generation rate, implantation time and annealing time were varied.

Previously, the mechanism for He transport and formation of intense swelling in tungsten was reported [12,13]. With the assumption that the binding energy of a He atom to a vacancy is so high that it never leave its substitutional site in the lattice, the diffusion coefficient of He atom in single crystal tungsten at 2100 °C was estimated to be 10^{-14} m^2/s; annealing at 2000 °C for 1 s would result in a He atom diffusion distance of 0.1 μm.

The implantation with 10^{19} He/m^2 followed by annealing at 2000 °C for 2 s resulted in the formation of a large number of tiny cavities in single crystal tungsten (Fig. 2(a)). Assuming that strong trap sites for He atoms are He-vacancy clusters only, each He atom would diffuse at most 0.2 μm away during annealing. In this case, almost all implanted He would remain in the matrix and/or form cavities with vacancies. Actually, the single step annealed single crystal tungsten indicated no cavities in the region from the surface to 1 μm in depth, supporting this model. On the other hand, no visible cavities were observed in the 1000 step annealed single crystal tungsten (Fig. 2(b)). The 1000 step He-implantation and annealing induced very small amount (10^{16} He/m^2) of He atoms and annealed at 2000 °C for 2 s in each step. In this case, almost all implanted He in each step could remain in matrix but probably not enough amount to form cavities with vacancies.

Single step annealing of polycrystalline tungsten also allowed implanted He atoms to remain in the matrix and form cavities just as the case for single crystal tungsten. The polycrystalline tungsten includes many grain boundaries, which could act as nucleation sites for cavities around the area He remained when grain boundary diffusion is not dominant. The existence of grain boundary actually led to significant cavity formation and greater cavity growth than in single crystal tungsten. The 1000 step implantation and annealing of polycrystalline tungsten resulted in no visible cavities observed. One of the reasons would be due to insufficient He amount in each step for cavity formation that is the same as the case of single crystal tungsten. The other possible reason is any recrystallization of the polycrystalline tungsten during annealing at 2000 °C for total 50 min.

Fig. 5 shows scanning electron microscope (SEM) images of polycrystalline tungsten as-implanted (a) and implanted with 10^{19} He/m^2 at 850 °C followed by annealing at 2000 °C in single step (b) and 1000 steps (c). As seen in Fig. 5(a), the average grain size of as-implanted polycrystalline tungsten is about 1 μm, while the polycrystalline tungsten implanted and annealed at 2000 °C in a single step indicated larger grain (3–10 μm in diameter). Fig. 5 shows that the 1000 step annealing of polycrystalline tungsten resulted in significant grain growth (30–50 μm in size). TEM samples prepared by FIB were 3×5 μm in size, meaning that the area observed did not include grain boundaries near the depth of He distribution. This would be the other reason why polycrystalline tungsten annealed in 1000 steps showed no visible cavities. However, the NRA results showed more He retention in polycrystalline tungsten compared to single crystal tungsten. This is probably because some of the implanted He remained in the matrix during recrystallization and formed cavities at around recrystallized grain boundaries.

5. Summary

The helium retention characteristics and helium bubble distribution of tungsten were studied using NRA and TEM for two forms of tungsten: single crystal and polycrystalline tungsten implanted to 1×10^{19} ^{3}He/m^2 and annealed at 2000 °C.

The NRA results revealed that as-implanted single crystal and polycrystalline tungsten exhibited similar helium retention characteristics. Stepwise annealing reduced the helium retention in both single crystal and polycrystalline tungsten when the number of implantation steps and annealing time were increased. The helium retention in single crystal tungsten dropped by 95% of the single step implantation (only 5% of He was retained). For the polycrystalline tungsten the reduction was 75%, with only 30% injected He retained. The TEM results indicated that the microstructure played a large role in helium trapping; the existence

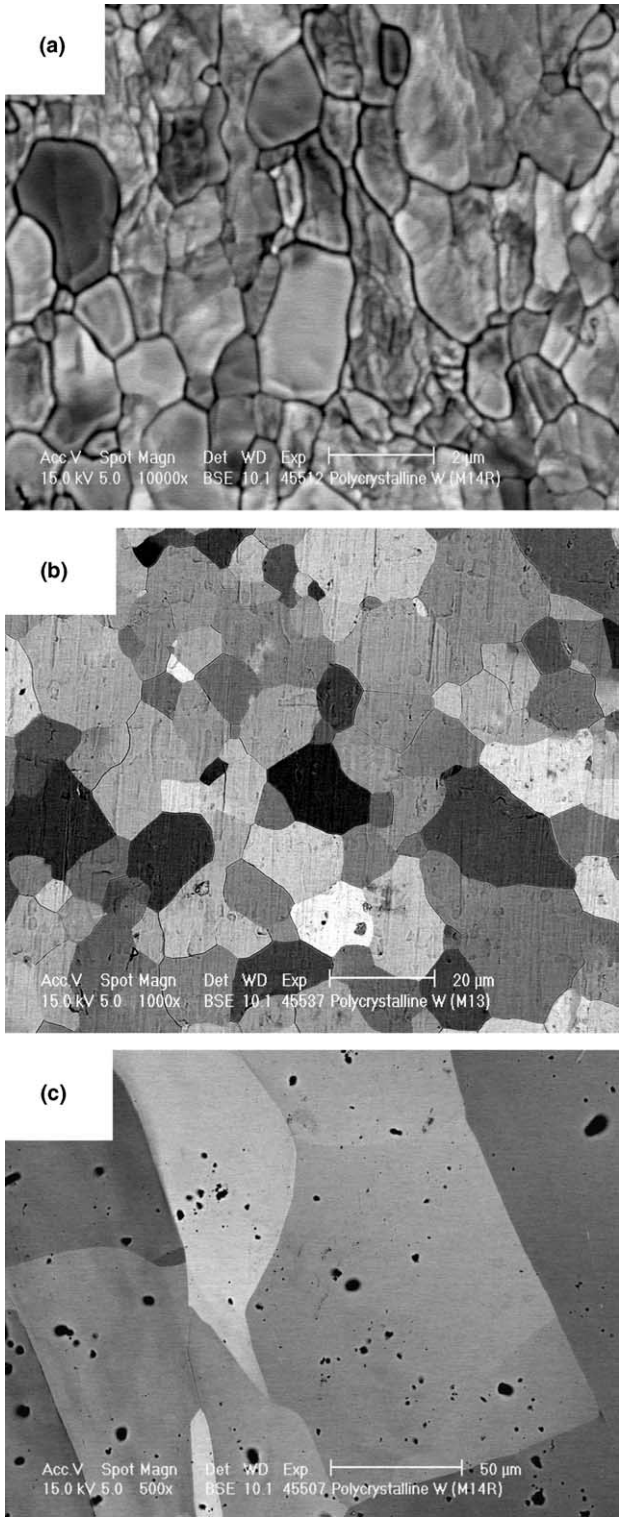

Fig. 5. SEM micrographs polycrystalline tungsten (a) as-implanted and implanted with 10^{19} He/m^2 at 850 °C followed by annealing to 2000 °C in (b) single step and (c) 1000 steps.

of grain boundaries, which act as strong nucleation sites for cavities, led to significant cavity formation and greater cavity growth. Single crystal tungsten had less trapping sites for helium, allowing long range He diffusion during annealing. This is probably the reason for less He retention in single crystal tungsten. The decrease of He retention in polycrystalline tungsten during multistep annealing may be due to significant recrystallization and grain growth, resulting in decrease of grain boundary density.

Acknowledgment

This research was sponsored by the US Department of Energy High Average Power Laser Program, under contract No. DE-AC05-00OR22725 with UT-Battelle, LLC.

References

[1] S.J. Zinkle, Gas assisted cavity formation and blistering in ceramics, in Fusion Materials Semiannual Progress Report for Period ending 30 June 2000, DOE/ER-0313/28 (1998) p. 187.
[2] G.M. McCracken, Rep. Prog. Phys. 38 (1975) 241.
[3] K.L. Wilson, Nucl. Fus. (1984) 85 (Special issue).
[4] E.L. Fleischer, M.G. Norton, Heterogen. Chem. Rev. 3 (1996) 171.
[5] H. Iwakiri, K. Yasunaga, K. Morishita, N. Yoshida, J. Nucl. Mater. 283–287 (2000) 1134.
[6] W.H. Geist, The $^{3}He(d,p)^{4}He$ reaction at low energies: Doctoral Dissertation, UNC-Chapel Hill, 1998.
[7] S. Gilliam, S. Gidcumb, N. Parikh, B. Patnaik, J.D. Hunn, L.L. Snead, J. Nucl. Mater., submitted for publication.
[8] A.A. Haasz, J.W. Davis, M. Poon, R.G. Macaulay-Newcombe, J. Nucl. Mater. 258–263 (1998) 889.
[9] M. Kaminsky, Radiation Effects on Solid Surfaces, American Chemical Society, Washington, DC, 1986.
[10] K. Shinohara, A. Kawakami, S. Kitajima, Y. Nakamura, M. Kutsuwada, J. Nucl. Mater. 179–181 (1991) 246.
[11] H. Iwakiri, H. Wakimoto, H. Watanabe, N. Yoshida, J. Nucl. Mater. 258–263 (1998) 873.
[12] V.N. Chernikov, A.P. Zakharov, J. Nucl. Mater. 165 (1989) 89.
[13] V.N. Chernikov, Ju.V. Lakhotkin, H. Ullmaier, H. Trikaus, P. Jung, H.J. Bierfeld, J. Nucl. Mater. 212–215 (1994) 375.